Vol. 45, No. 3 (2023) 472-486, DOI: 10.24874/ti.1466.03.23.05

Tribology in Industry

www.tribology.rs

RESEARCH

Effects of Shot Peening Pressure on Friction and Wear of High Pressure Cold Sprayed Ti-6Al-4V Coatings Under Dry and Lubrication Conditions

Nay Win Khun[a,b,*], Pham Quang Trung[c], Adrian Wei YeeTan[a,b], Wen Sun[a,b], Erjia Liu[a,b], David Lee Butler[d]

[a]*Rolls-Royce@NTU Corporate Lab, Nanyang Technological University, 50 Nanyang Avenue, Singapore 639798, Singapore,*
[b]*School of Mechanical and Aerospace Engineering, Nanyang Technological University, 50 Nanyang Avenue, Singapore 639798, Singapore,*
[c]*Department of Materials Processing Technology, Ho Chi Minh City University of Technology, VNU-HCM, Ho Chi Minh City, Vietnam,*
[d]*Department of Design Manufacture and Engineering Management, University of Strathclyd, Glasgow G1 1XJ, United Kingdom.*

Keywords:

Cold spray
Shot peening
Ti64 coating
Microstructure
Hardness
Wear

* Corresponding author:

Nay Win Khun
E-mail: khunnaywin@gmail.com

Received: 26 March 2023
Revised: 3 May 2023
Accepted: 20 May 2023

A B S T R A C T

The effects of shot peening pressure (SPP) (10-60psi) on the wear resistance of high-pressure-cold-sprayed Ti-6Al-4V coatings (HPCSTi64-Coats) were investigated against 100Cr6 steel with or without mineral oil lubricant (MOL), which have not been reported yet. The specific wear rate (SWR) of the HPCSTi64-Coat with the SPP of 60psi was 29% lower than that of the one without shot peening (SP). With the MOL, the SWR of the HPCSTi64-Coat without SP was 40.8% higher than that of the one with 10psi. The SWR of the HPCSTi64-Coat became higher with higher SPP while the SWR of the HPCSTi64-Coat with 60psi was 76.5% higher than that of the one with 10psi. Therefore, the best SPP for the best bearing surface of the HPCSTi64-Coat with the MOL was 10psi. In spite of that, the HPCSTi64-Coats lubricated with the MOL had smaller SWRs for all the SPPs so that the SWRs of the HPCSTi64-Coats with the SPPs of 0 and 60psi were 2.4 and 0.9 times higher, respectively, in the tribo-tests without than with the MOL.

1. INTRODUCTION

In aerospace industry, Ti-6Al-4V (Ti64), which has good machinability, good mechanical properties and light weight, is tirelessly used to make aircraft components [1-3]. Low abrasive wear resistance of Ti64, however, can lead to physical damages of Ti64 based aircraft components in their long-service so such damaged expensive components are necessarily repaired using traditional high-temperature-repair-technologies such as thermal-spraying and welding [3-5]. Unfortunately, the high-temperature-repair-technologies create intrinsic

problems in built metallic materials such as high porosity level, thermal residual stress and oxidation level, limiting production of high quality metallic materials [4,6,7]. For these reasons, nowadays, low temperature cold spray (CS) repair technology is progressively interested in aerospace industry to repair damages of aircraft components with metallic materials having low porosity and oxidation levels and lack of thermal residual stress [4,8,9]. Some researchers have proved the potential of low temperature CS repair technology for repair application [2,4,8,9]. Nevertheless, the CS technology is still at a research and development stage, and its private nature prevents willingness of researchers and developers to disclose their findings [4]. The tribological data of HPCSTi64-Coats are therefore very limited in the literature.

HPCSTi64-Coats have intrinsic porous-structures, although their porosity levels are relatively low compared to those of thermal-sprayed coatings, which are prone to fatigue damages in service since the fatigue failures originate from surface defects, such as dents, voids, pores, interstitial weakness sites, poor particle bonding sites and so on, associated with CS processes [2,4,8-10]. In aerospace industry, it is widely accepted that the fatigue resistance of aircraft components can be effectively improved by SP surface treatment via basic modification of their surface microstructure, texture, topography and hardness, near-surface dislocation and residual stress [10-13]. Some researchers reported that SP of metallic materials could promote their surface abrasive wear resistance via their enhanced surface hardness [10,11]. It is therefore supposed that SP of HPCSTi64-Coats could lessen their surface defects for their better fatigue resistance and surface abrasive wear resistance. The data on the abrasive wear resistance of HPCSTi64-Coats with SP have not been widely disclosed in the literature. In addition, SP process has a complex nature with its different process parameters [10-13]. Therefore, the tribological properties of HPCSTi64-Coats with SP should be comprehensively researched.

Recently, Khun et al. [11] investigated the tribological properties of commercial AA7075-T6 shot peened at different SPPs of 10-60psi with MOL, and revealed that the AA7075-T6 had the best bearing surface at 60psi. Since Ti64 is generally harder than AA7075-T6, SP of Ti64 can give rise to its different surface features and thereby affect its bearing surface. As a result, a variation in the best bearing surfaces of HPCSTi64-Coats with their SP-induced-surface-features should be systematically investigated with MOL. Such data of HPCSTi64-Coats have not been found in the literature yet. It is clear that the effects of shot peening pressure on the friction and wear of HPCSTi64-Coats against 100Cr6 steel without or with MOL have not been reported yet.

In this investigation, the surfaces of HPCSTi64-Coats were mechanically treated with SP at different SPPs of 10-60 psi with 10psi interval. Changes in their surface microstructure, roughness, porosity level and hardness with SPP were studied. Their frictional and wear behavior against 100Cr6 steel without or with MOL were carefully examined with respect to SPP. Correlation between their surface features and tribological properties was studied in order to understand the influence of SP-induced-surface-features on their frictional and wear behavior. Their best bearing surfaces with MOL were evaluated with respect to SPP.

2. EXPERIMENTAL DETAILS

2.1 Sample preparation

A HPCS system with a series of PCS-1000 was applied to spray Ti64 powder (PG-AMP-1120) with a size distribution of 1-45 μm (Figure 1) on commercially available Grade 5 Ti64 substrates (Titan Engineering) with 50 mm × 50 mm × 8 mm. Apparent oxygen (O) on the spray Ti64 powder was not detected in its EDX specturm with main peaks of titanium (Ti), aluminum (Al) and vanadium (V) although adsorbed carbon (C) on the powder was found (Figure 1b). The CS process parameters were optimized with gas-temperature of 950°C, gas-pressure of 2.5 MPa, nozzle-speed of 100-400 mm/s, spray-angle of 90°, stand-off distance of 25 mm and step-distance of 1 mm. The working-gas was helium (He). The HPCSTi64-Coats had relatively uniform thickness of 3 mm in Figure 2.

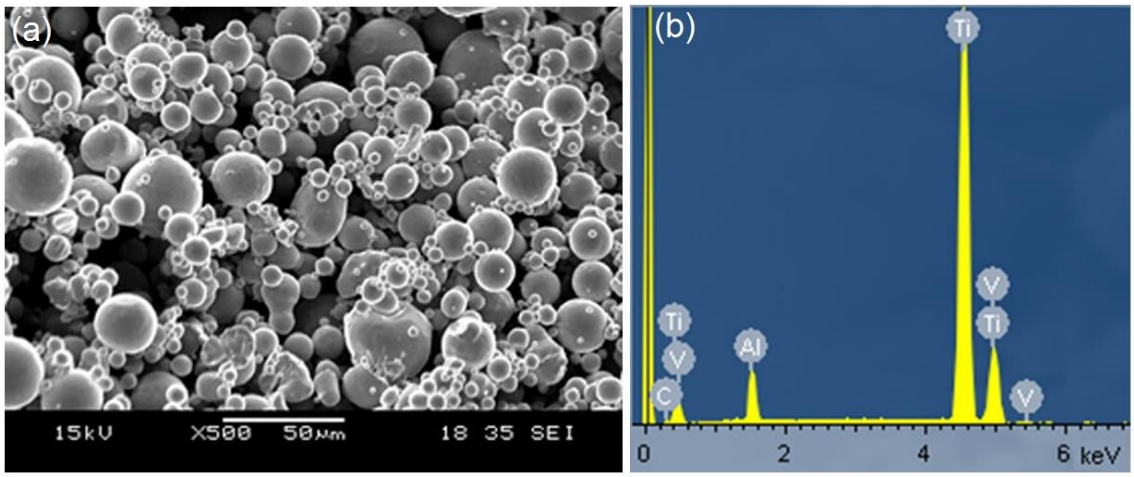

Fig. 1. (a) Overview of spray Ti64 powder used in this study and (b) its EDX spectrum.

Fig. 2. (a) Top and (b) cross-sectional views of as-deposited HPCSTi64-Coat with about 3 mm thickness on Ti64 substrate.

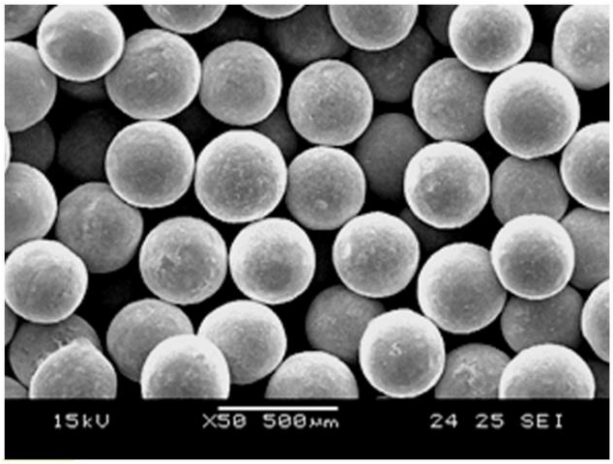

Fig. 3. SEM micrograph of spherical S110 steel-shots.

The SP of HPCSTi64-Coats was carried out using air blast SP equipment of Abrasive Engineering Pte. Ltd. with nozzle-diameter of 14 mm at impact-angle of 80°, rotating-table-speed of 1°/s, media-flow-rate of 3 kg/min and nozzle-speed of 150 mm/s at different SPPs of 10-60psi (68.9-413.7kPa) [10,11]. The shots used for the SP were S110 steel solid-spheres with a mean diameter of 300µm and hardness of 500±30Hv, and they had smooth surfaces with an uniform size distribution as found in Figure 3. The surfaces of HPCSTi64-Coats were mechanically polished with 1200 grit papers at the final-stage before SP.

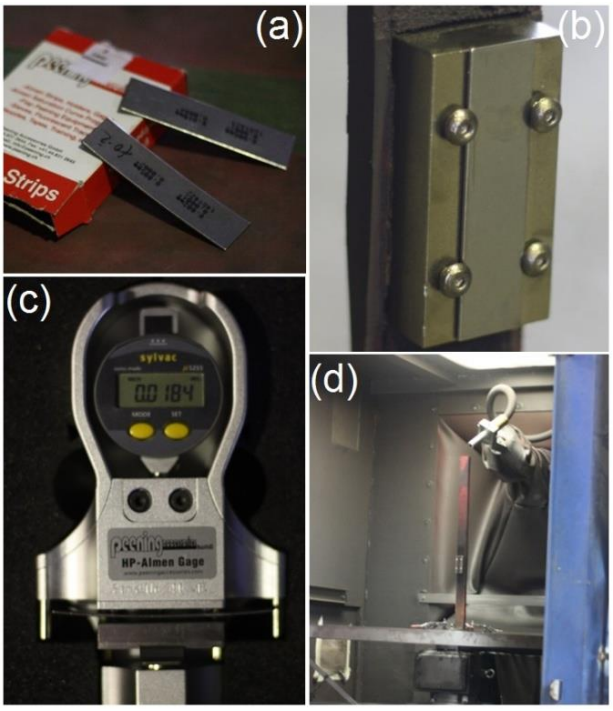

Fig. 4. (a) Almen strip, (b) Almen strip mounted on holding-fixture, (c) Almen guage and (d) mounted sample in SP chamber.

In the SP with various cycle T, standard Almen SAE 1070 strip of Peening Accessories (Figure 4a) with a size of 76.1 mm × 18.95 mm × 1.29 mm was removed from a holding-fixture (Figure 4b) and its arc-height was measured using Almen gauge of Peening Accessories (Figure 4c) to plot its maximum arc-height with respect to exposure time using PA[2] software to determine the SP intensity (SPI). Then, the HPCSTi64 samples were mounted in the same fixture to get shot peened in the SP chamber (Figure 4d) under the same conditions for 20 s that was longer than the time required to reach a saturation point where the arc-height of the almen strip was stabilized. A series of tests were conducted to measure SPIs at different SPPs. Table 1 shows the SPIs measured at SPPs of 10-60psi.

Table 1: SPIs measured at different SPPs.

Shot peening pressure (psi)	Shot peening intensity
10	6.1A
20	7.2A
30	8.3A
40	9.9A
50	11.1A
60	12.1A

2.2. Characterization

Scanning electron microscopy (SEM) with a series of JEOL-JSM-5600LV was applied to capture the micrographs of spray Ti64 powder, spherical S110 steel shots and wear debris and the SP surface and wear morphologies of the HPCSTi64-Coats.

The surface and cross-sectional microstructures of the HPCSTi64-Coats were observed using optical microscopy (OM). Prior to the OM observation, epoxy molded HPCSTi64-Coats were polished to achieve their mirror-like surfaces, and then etched with Kroll's reagent for their detailed microstructures [3,4]. The wear scars of the worn 100Cr6 steel balls were captured by the OM immediately after the tests were completed.

The OM microstructures of the HPCSTi64-Coats, captured with a lowest magnification 5× lens before getting etched, were analyzed using Image "J" software to evaluate their surface porosity levels. Six OM micrographs of each HPCSTi64-Coat were used to calculate its averaged surface porosity level.

The 3D surface roughness parameters (arithmetic average (S_a) and root mean squared (S_q) surface roughnesses, maximum peak height (S_p) and valley depth (S_v), and surface skewness (S_{sk}) and kurtosis (S_{ku})) of the HPCSTi64-Coats were obtained with 3D surface profilometry (3DSP) with a series of Talyscan 150 by scanning in a scan area of 1mm×1mm with a 4 μm diamond stylus in a contact mode. Three 3D surface topographies of each HPCSTi64-Coat were used to calculate its averaged 3D surface roughness parameters.

A Vickers micro-indenter with a series of Future-tech FM-300e was applied to make six random indentations on the surface of each HPCSTi64-Coat under a normal load of 50 g (0.49 N) to calculate its averaged surface hardness.

The wear tracks of the HPCSTi64-Coats were generated rotating against fixed 6 mm 100Cr6 steel balls in a circular-path of 2 mm in diameter for 30000 laps (about 189 m) at a sliding speed of 3 cm/s under an applied normal load of 1 N while their friction coefficients were simultaneously measured using a ball-on-disc micro-tribological test (CSM) conformed to standards of DIN50324 and ASTM G99. The 3D wear tracks in a size of 1.5mm×0.5mm were scanned using the 3DSP to evaluate the wear widths and depths with three-five measurements per wear track. The wear width and depth were averaged from the three-five measurements (per wear track), which were used to calculate the SWR that was the wear volume divided by the product of the normal load and the sliding distance [3,14]. Three wear tracks of each HPCSTi64-Coat were counted for its averaged SWR. For the tribological tests under lubrication condition, the ACROS MOL with a laboratory grade was used.

3. RESULTS AND DISCUSSION

The polished HPCSTi64-Coat has a relatively smooth surface with S_a of 0.21 μm and S_q of 0.26 μm as found in Figures 5a and b. Such smooth surfaces were shot peened at different SPPs.

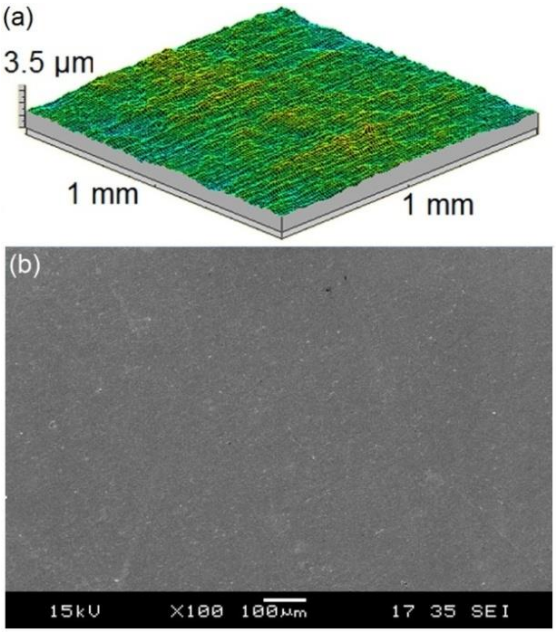

Fig. 5. Surface (a) topography and (b) morphology of polished HPCSTi64-Coat captured before SP

The SP surface topographies and morphologies of the HPCSTi64-Coats with different SPPs are presented in Figure 6. The SP at 10psi apparently forms dimples on the surface of the HPCSTi64-Coat with a full-coverage for its rougher surface as found in the comparison of Figures 5 and 6a. In Figures 6a-f, the surface dimples become larger and deeper with higher SPP via the more energetic bombardment of steel shots so that the formation of deepest surface dimples with the highest SPP of 60psi results in the most protruded surface asperities for the highest surface roughness of the HPCSTi64-Coat (Figure 6f) [10,11]. Therefore, the largest S_p and S_v values of the HPCSTi64-Coat are consistently found at the highest SPP of 60psi while the S_a and S_q values at 60psi are 8.9 and 9.1 times larger than those at 0psi, respectively (Table 2).

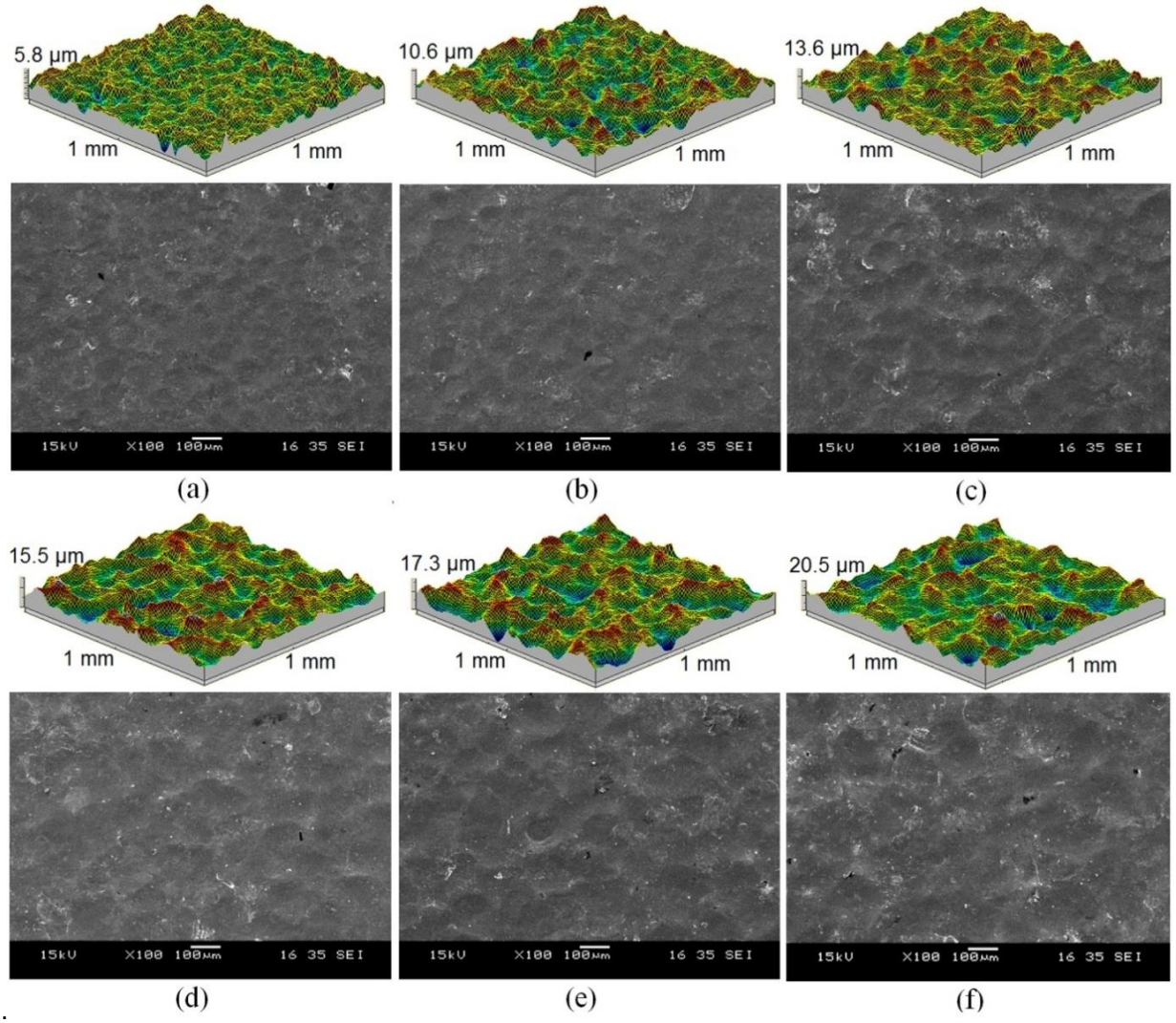

Fig. 6. Surface topographies (above) and morphologies (below) of HPCSTi64-Coats with SPPs of (a) 10, (b) 20, (c) 30, (d) 40, (e) 50, and (f) 60psi.

Table 2: 3D S_a, S_q, S_p and S_v of HPCSTi64-Coats without or with SP at different SPPs.

	Shot peening pressure (psi)						
	0	**10**	**20**	**30**	**40**	**50**	**60**
S_a (µm)	0.21±0.13	0.43±0.04	0.92±0.13	1.22±0.04	1.47±0.19	1.71±0.14	1.86±0.11
S_q (µm)	0.26±0.15	0.56±0.04	1.17±0.16	1.55±0.04	1.86±0.25	2.18±0.15	2.36±0.15
S_p (µm)	2.53±0.54	3.34±0.81	5.05±0.55	6.03±0.82	7.14±0.59	7.24±1.11	9.15±1.66
S_v (µm)	2.79±2.02	3.22±0.48	5.11±0.27	6.5±1.23	7.13±1.14	8.35±1.32	9.31±2.13

The S_{sk} and S_{ku} values of the HPCSTi64-Coat without SP are in the ranges of -1.98 to -2.04 and 4.02 to 5.63, respectively, while the S_{sk} and S_{ku} values of the the HPCSTi64-Coat with the SPP of 10psi are in the ranges of -0.395 to -0.425 and 3.06 to 3.42, respectively. The HPCSTi64-Coat has intrinsic pores in its surface microstructure. The number of intrinsic pores can be lessened by the energetic bombardment of steel shots during the SP. Therefore, the smaller negative S_{sk} value of the HPCSTi64-Coat with 10psi compared to that of the one without SP implies that the HPCSTi64-Coat with 10psi has a bearing surface with a smaller number of intrinsic deep pores [15-17]. In addition, the smaller S_{ku} value of the HPCSTi64-Coat with 10psi indicates that it has a broader height distribution of peaks on its surface for its better bearing surface [15-17].

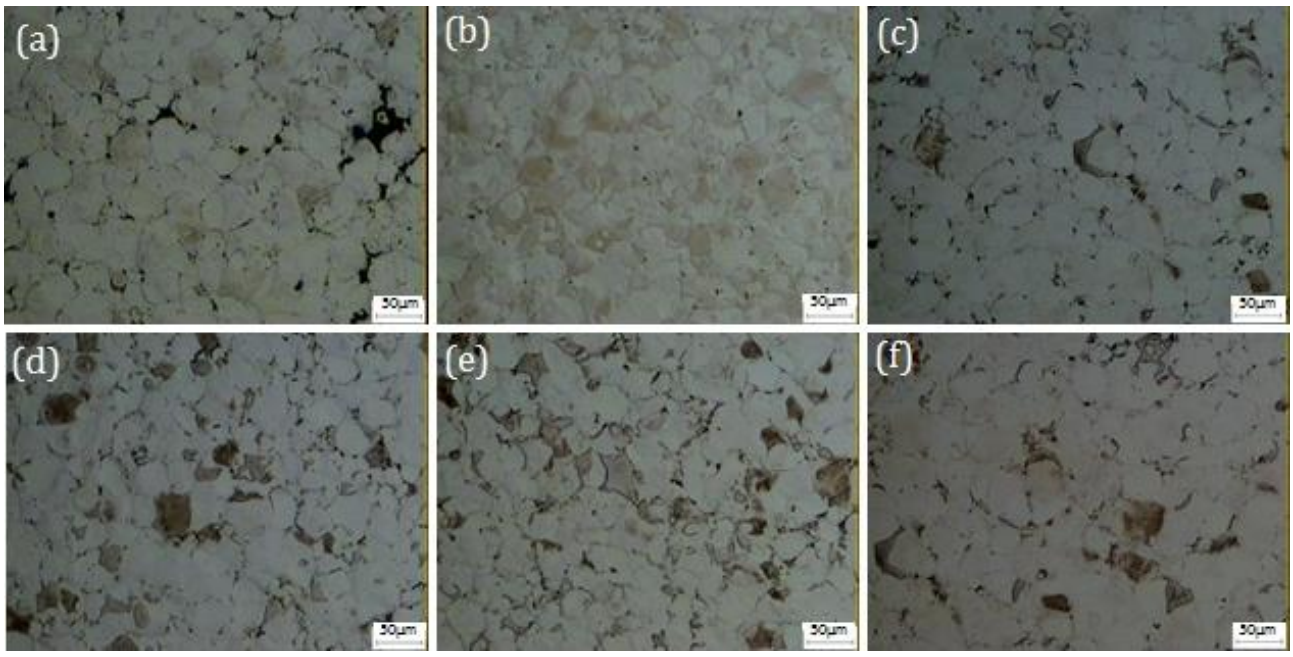

Fig. 7. Surface microstructures of HPCSTi64-Coats with SPPs of (a) 0, (b) 10, (c) 20, (d) 30, (e) 50 and (f) 60psi.

Increasing the SPP to 60psi systematically shifts the S_{sk} values of the HPCSTi64-Coats to more positive values of 0.01-0.02 while their S_{ku} values increase to 3.53-3.83. Since the surface has a lot of peaks if S_{sk}> 0 [11,15-17], the HPCSTi64-Coats with higher SPPs have the surfaces with a larger number of peaks. The larger S_{ku} values than "3" of the HPCSTi64-Coats for all the SPPs indicate that the HPCSTi64-Coats with SP have a narrow height distribution of peaks on their surfaces [11,15-17]. However, the smaller S_{ku} values of the HPCSTi64-Coats with lower SPPs are indicative of the broader height distribution of peaks on their surfaces for their better bearing surfaces [11,15-17]. It can be deduced that the HPCSTi64-Coat with the lowest SPP of 10psi has the best bearing surface among the HPCSTi64-Coats used in this study as well as the better bearing surface than the one without SP. The bearing surface is essential for an effective lubrication.

In our previous study on AA 7075-T6 with MOL [11], its best bearing surface was achieved at the highest SPP of 60psi. However, in this study, the best bearing surface of the HPCSTi64-Coat is found at the lowest SPP of 10psi. Such different

results clearly imply that a difference in the hardness of metallic materials results in forming different surface features during SP for different bearing surfaces.

The surface porosity levels of the HPCSTi64-Coats with different SPPs are 1.72±0.52% for 0psi, 0.52±0.29% for 10psi, 0.68±0.33% for 20psi, 0.82±0.34% for 30psi, 0.55±0.21% for 40psi, 0.94±0.15% for 50psi, and 0.83±0.28% for 60psi, indicating that the HPCSTi64-Coats with SP have the lower surface porosity levels than the one without SP.

Figure 7 shows the surface microstructures of the HPCSTi64-Coats with different SPPs. In the surface microstructure of the HPCSTi64-Coat without SP (Figure 7a), nearly circular shaped Ti64 particles with visible interfaces are found as a significant number of intrinsic pores apparently exist. However, the HPCSTi64-Coats with different SPPs (Figures 7b-f) have surface microstructures with a smaller number of pores, indicating that the SP lessens the surface porosity level via the further deformation of sprayed Ti64 particles. Therefore, the HPCSTi64-Coats with different SPPs have sprayed Ti64 particles with less circularity in their surface microstructures than the one without SP because the severely deformed Ti64 particles during the SP have more irregular shapes.

Figure 8 shows the cross-sectional microstructures of the HPCSTi64-Coats with different SPPs. During the SP, the SP causes a shock wave which in turn results in the further deformation of sprayed Ti64 particles [18,19]. Since a more intense shock wave associated with higher SPP can go deeper into a sub-surface region, the SP at a higher SPP results in a deeper affected region. Therefore, the affected region of the HPCSTi64-Coats becomes deeper with higher SPP as found in Figures 8a-c.

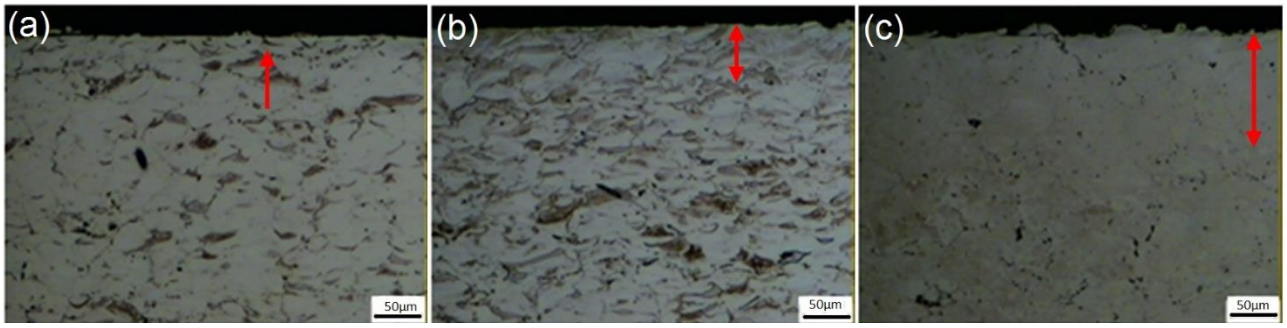

Fig. 8. Cross-sectional microstructures of HPCSTi64-Coats with SPPs of (a) 10, (b) 30 and (c) 60psi. The red arrows show affected areas.

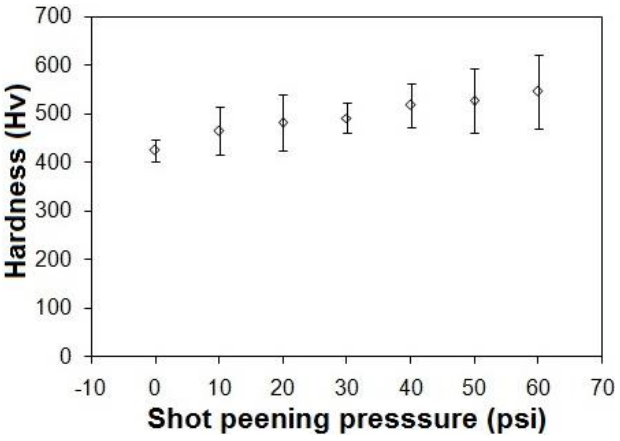

Fig. 9. Surface hardness of HPCSTi64-Coats with respect to SPP.

Figure 9 presents the surface hardness of the HPCSTi64-Coats as a function of SPP. The surface hardness of the HPCSTi64-Coat is increased from 424.3 Hv to 545.7 Hv by increasing the SPP from 0 to 60psi. Such 28.6% increment in the surface hardness is probably a result of the promoted cold work hardening associated with the increased energetic bombardment of steel shots [10-12,20,21].

Figure 10a presents the friction coefficients of the HPCSTi64-Coats tested without or with the MOL as a function of SPP. Under the dry condition, increasing the SPP from 0 to 60psi slightly increases the friction coefficient of the HPCSTi64-Coat from 0.51 to 0.55 because its increased surface roughness increases mechanical interlocking between asperities of two rubbing surfaces, which is consistent with our previous reports [10,11,22-24].

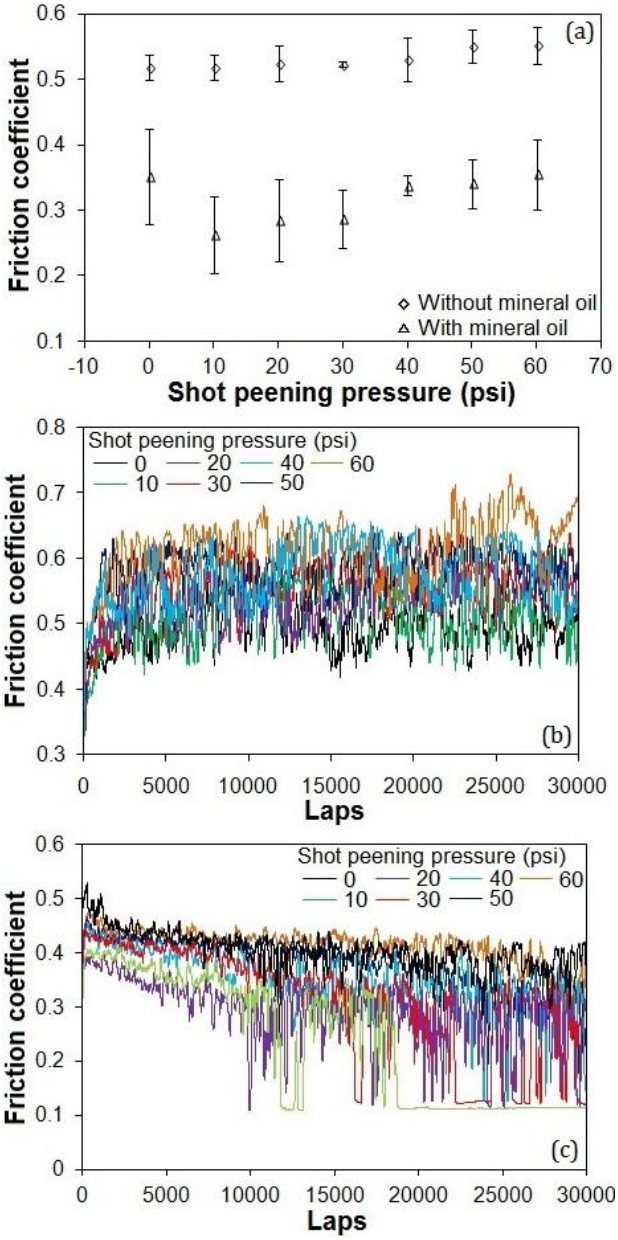

Fig. 10. (a) Friction coefficients of HPCSTi64-Coats tested without or with MOL as a function of SPP, and (b and c) friction coefficients of HPCSTi64-Coats with different SPPs tested (b) without and (c) with MOL as a function of the number of laps.

Under lubrication with the MOL, the friction coefficient of the HPCSTi64-Coat without SP is 0.35 that is 31.4% lower than that of the same one tested dry. The friction coefficient of the HPCSTi64-Coat with the SPP of 10psi is 0.26 that is 25.7% lower than that of the one without SP as a result of its better bearing surface for the more effective lubrication with the MOL [10,11,25,26]. However, the friction coefficient of the HPCSTi64-Coat increases to 0.36 with increased SPP to 60psi, implying that its increased surface roughness still can affect its friction even under the lubrication condition. It is clear that the HPCSTi64-Coat with 10psi exhibits the lowest friction with the MOL among the HPCSTi64-Coats used in this study due to its best bearing surface. The MOL is an effective lubricant for the HPCSTi64-Coats so that all the HPCSTi64-Coats without or with SP have the lower friction under the lubrication condition as found in Figure 10a.

Figure 10b illustrates the trends of friction coefficient versus laps of the HPCSTi64-Coats with different SPPs tested dry in which the HPCSTi64-Coats with the SPPs of 10 and 60psi exhibit the lowest and highest friction throughout the wear-tests, respectively. It is found that the stick-slip phenomena caused by the sliding of the hard steel ball on the HPCSTi64-Coat causes a significant fluctuation in the trends of friction coefficient versus laps [4,10,11,27].

The trends of friction coefficient versus laps of the HPCSTi64-Coats with different SPPs lubricated with the MOL are presented in Figure 10c, in which an employment of the MOL lessens the stick-slip phenomena as well as causes stable wear during the entire sliding. The friction coefficient of the HPCSTi64-Coat with the SPP of 10psi steadily decreases with increased laps at the beginning, and then dramatically drops and becomes stable at the much lower values, indicating that the HPCSTi64-Coat achieves the better condition of its bearing surface after the prolonged sliding of the steel ball wears out the coating surface asperities. The similar behavior was observed in all the three-time-measurements of the same sample. Achieving the better condition of the best bearing surface during the prolonged sliding is mainly responsible for the lowest trend of friction coefficient versus laps of the HPCSTi64-Coat with 10psi. It is found in Figure 10c that the higher surface roughness of the HPCSTi64-Coat associated with higher SPP gives rise to its higher friction throughout the wear-test so that the HPCSTi64-Coat with the highest SPP of 60psi has the highest trend of friction coefficient versus laps.

The SWRs of the HPCSTi64-Coats with different SPPs tested without or with the MOL are presented in Figure 11. The SWR of the HPCSTi64-Coat tested dry decreases from

93.9×10^{-14} m^3/(Nm) to 66.7×10^{-14} m^3/(Nm) with increased SPP from 0 to 60psi. Such 29% decrement in the SWR clearly indicates that increasing the SPP increases the wear resistance of the HPCSTi64-Coat by increasing its surface hardness [10-12]. The lower SWRs of all the HPCSTi64-Coats with SP than that of the one without SP confirm that the SP promotes the surface wear resistance of the HPCSTi64-Coats under the dry condition.

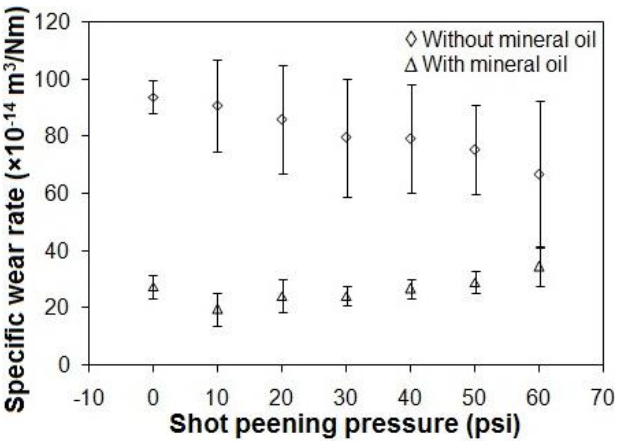

Fig. 11. SWRs of HPCSTi64-Coats tested without or with MOL as a function of SPP.

In Figure 11, the SWR of the HPCSTi64-Coat without SP lubricated with the MOL is 27.6×10^{-14} m^3/(Nm) that is 70.6 % lower than that of the same one tested dry. The SP of the HPCSTi64-Coat at 10psi gives rise to the 29% lower SWR of 19.6×10^{-14} m^3/(Nm) than the one without SP because the MOL more effectively lubricates the better bearing surface of the HPCSTi64-Coat with 10psi [11,25,26]. However, the SWR of the HPCSTi64-Coat increases to 34.6×10^{-14} m^3/(Nm) with increased SPP to 60psi because the degraded bearing surface of the HPCSTi64-Coat with increased SPP is responsible for its increased wear under the lubrication condition. It reveals that the bearing surface of the HPCSTi64-Coat is the more significant effect on its wear under the lubrication condition compared to the cold work hardening effect mainly seen under the dry condition. It is therefore clear that the HPCSTi64-Coat with the best bearing surface associated with the SPP of 10psi shows its lowest wear with the MOL in this study. The lower wear of the HPCSTi64-Coats lubricated with the MOL for all the SPPs confirms that the MOL is an effective lubricant for the HPCSTi64.

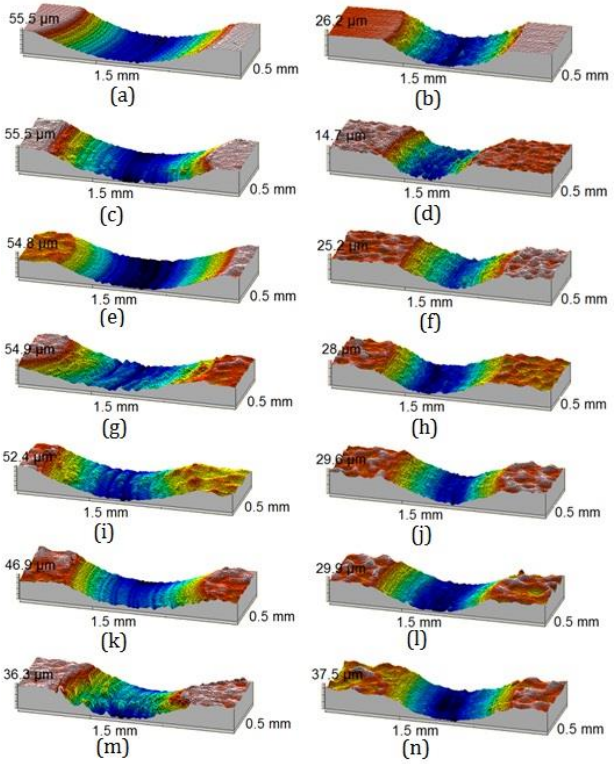

Fig. 12. 3D wear topographies of HPCSTi64-Coats with SPPs of (a and b) 0, (c and d) 10, (e and f) 20, (g and h) 30, (i and j) 40, (k and l) 50, and (m and n) 60 psi, tested (a, c, e, g, i, k and m) without or (b, d, f, h, j, l and n) with MOL.

Figures 12 shows the 3D wear topographies of the HPCSTi64-Coats with different SPPs tested without or with the MOL. In Figure 12a, the dry sliding of a steel ball on the HPCSTi64-Coat without SP generates an apparent wear track on the coating surface. The wear track of the HPCSTi64-Coat tested dry becomes smaller with higher SPP as a result of its higher wear resistance as found in Figures 12a, c, e, g, i, k and m. In Figures 12b, d, f, h, j, l and n, the wear tracks of the HPCSTi64-Coats lubricated with the MOL are apparently smaller than those of the ones tested without the MOL for all the SPPs due to the effective-lubricating-effect of the MOL. The lowest wear of the HPCSTi64-Coat lubricated with the MOL results in the smallest wear track on its SP surface at 10psi. The bottom surface roughness of the wear tracks tested with the MOL are less for most of the SPPs compared to those of the ones tested without the MOL, which could be correlated to the less stick-slip phenomena occured during the sliding with the MOL for the smaller fluctuation in the friction coefficients with respect to the number of laps.

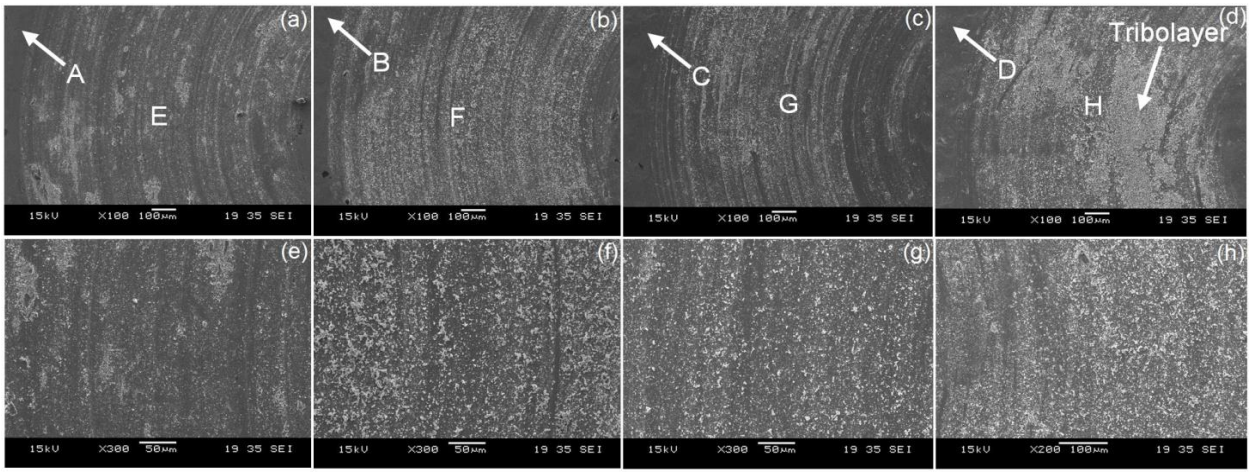

Fig. 13. Wear morphologies of HPCSTi64-Coats with SPPs of (a and e) 0, (b and f) 10, (c and g) 50, and (d and h) 60psi, tested without MOL, observed at different magnifications.

The SEM micrographs showing the wear morphologies of the HPCSTi64-Coats with different SPPs tested dry are presented in Figure 13, in which the smaller wear tracks are consistently found at the higher SPPs. Abrasive-lines are apparently found on the wear tracks of all the HPCSTi64-Coats with different SPPs while wear debris generated via abrasive wear are found on all the wear tracks [3,10,11,28-30]. It is clear that the abrasive wear is the main contributor to the wear of the HPCSTi64-Coats tested against the steel balls under the dry condition. The formation of tribo-layers is found on the wear tracks of the HPCSTi64-Coats expecially for the higher SPPs. Generally, tribo-layers are formed by a compaction of wear debris during repeated sliding [10,11,31]. It is supposed that the improved wear resistance of the HPCSTi64-Coat associated with higher SPP allows more compaction of wear debris to form the tribo-layers that are somewhat harder. An existence of the tribo-layers on the wear track is also responsible for lessening the wear of the HPCSTi64-Coat with higher SPP.

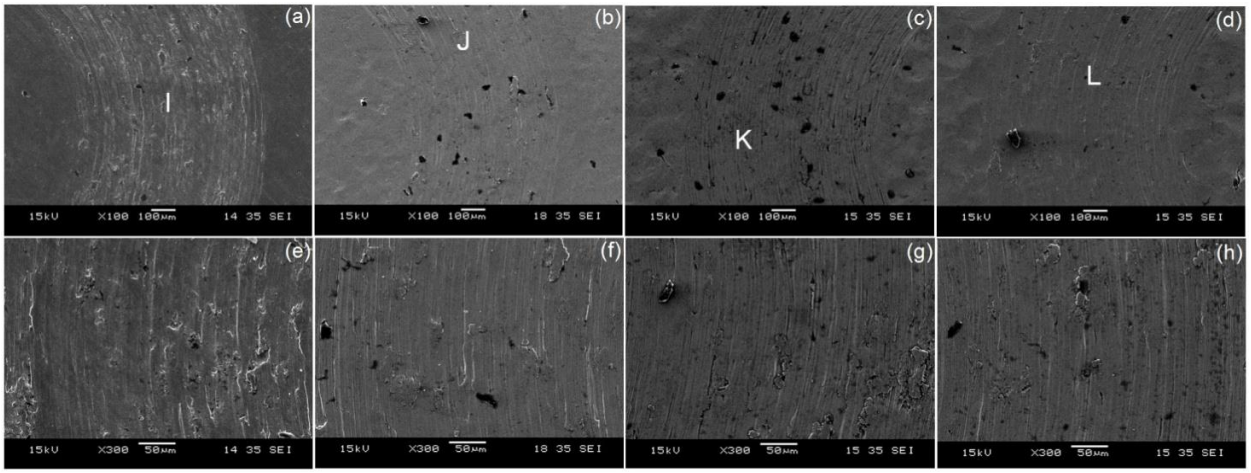

Fig. 14. Wear morphologies of HPCSTi64-Coats with SPPs of (a and e) 0, (b and f) 10, (c and g) 50, and (d and h) 60psi, tested with MOL, observed at different magnifications.

The SEM micrographs showing the wear morphologies of the HPCSTi64-Coats with different SPPs lubricated with the MOL are presented in Figure 14. The HPCSTi64-Coats lubricated with the MOL (Figure 14) have apparently smaller wear tracks compared to those tested dry (Figure 13). Abrasive wear debris are not apparently found on the wear tracks of the HPCSTi64-Coats lubricated with the MOL, indicating that the MOL effectivly lessens the abrasive wear of the HPCSTi64-Coats. However, some abrasive-lines are still found on the wear tracks of the HPCSTi64-Coats, which mean that the sliding of the steel balls still can generate the abrasive wear of the HPCSTi64-Coats even under the lubrication with the MOL.

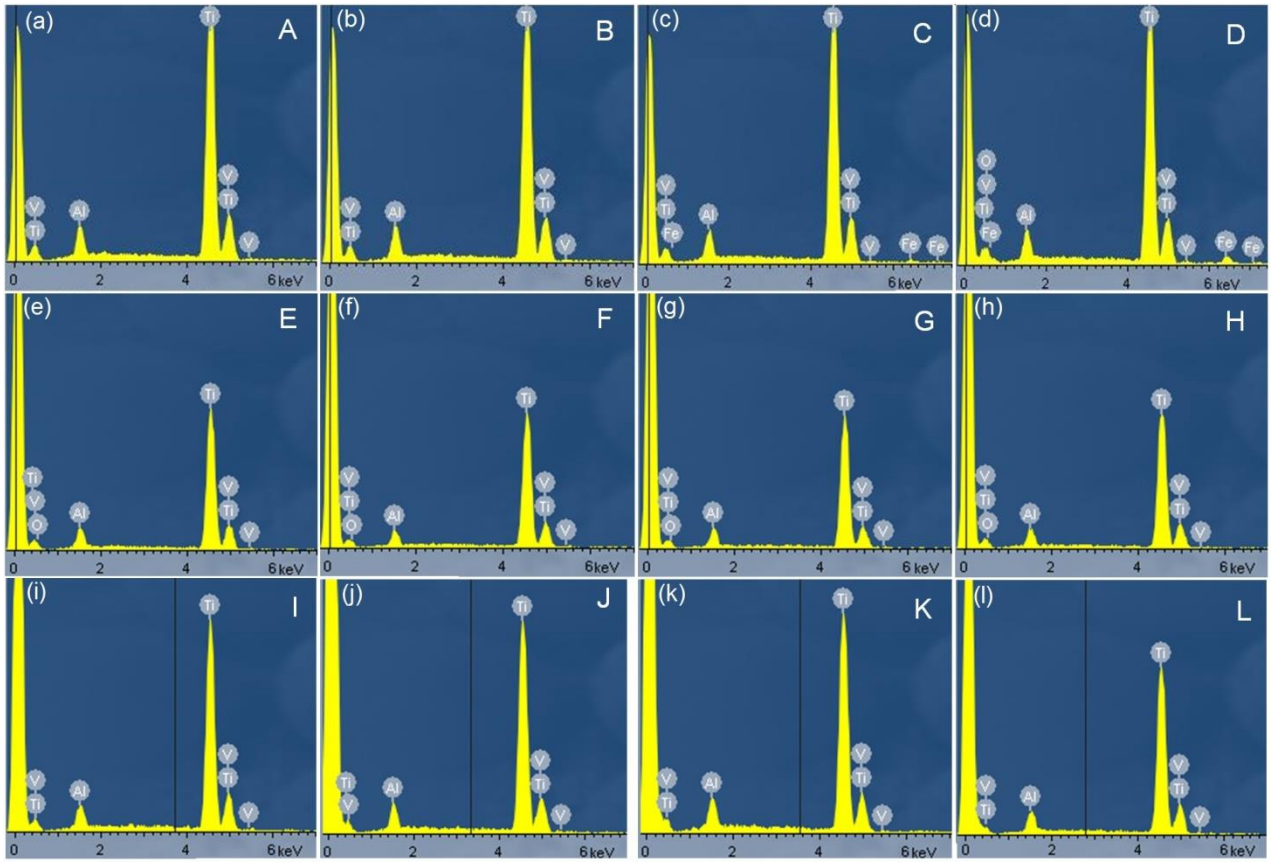

Fig. 15. EDX spectra of HPCSTi64-Coats with SPPs of (a, e and i) 0, (b, f and j) 10, (c, g and k) 50, and (d, h and l) 60psi, tested without (e, f, g and h) or (i, j, k and l) with MOL, measured at locations (a) "A" in untested area and (e) "E" in wear track of Figure 13a, (b) "B" in untested area and (f) "F" in wear track of Figure 13b, (c) "C" in untested area and (g) "G" in wear track of Figure 13c, (d) "D" in untested area and (h) "H" in wear track of Figure 13d, (i) "I" in wear track of Figure 14a, (j) "J" in wear track of Figure 14b, (k) "K" in wear track of Figure 14c and (l) "L" in wear track of Figure 14d.

In Figure 15a, the HPCSTi64-Coat without SP has Ti, Al and V peaks, mainly attributed to the Ti64 matrix, on the EDX spectrum of its untested area [3,11]. The HPCSTi64-Coats with the SPPs of 10-40psi have similar EDX spectra for their untested areas (Figure 15b) to that of the one without SP from which it can be seen that the SP at 10-40psi does not significantly change the surface chemistry of the HPCSTi64-Coats. When the SPP of 50psi is applied, the HPCSTi64-Coat has an additional iron (Fe) peak on the EDX spectrum of its untested area (Figure 15c). The Fe peak probably results from wear debris left by the wear of steel shots during the SP [10,11,28-30]. In addition to the Ti, Al, V and Fe peaks, an O peak is detected on the untested area of the HPCSTi64-Coat with the SPP of 60psi (Figure 15d). The high energetic bombardment of steel shots during the SP probably convert their impact energies into heat at their contact points to induce an oxidation process while the frictional heat generated at their contact points helps the oxidation process [10,11,28-30]. The energetic SP activates the surface of the HPCSTi64-Coat to have more interaction with surrounding oxygen [10,11]. These are the possible reasons why the O peak is detected on the surface of the HPCSTi64-Coat with 60 psi. In Figures 15e-h, the HPCSTi64-Coats without or with SP have similar EDX spectra measured on their wear tracks, implying that they have similar wear mechanisms duing the tribo-tests without the MOL. The EDX spectra measured on the wear tracks (Figures 15e-h) have an additional O peak compared to those detected on the untested areas (Figures 15a-d), and the O peak is attributed to the dry-sliding-induced-oxidation-process [3,10,11,28-30]. However, the O peaks are not found on the EDX spectra of the wear tracks lubricated with the MOL (Figures 15i-l) because an employment of the MOL during the sliding suppresses the generation of fricitonal heat that is responsible for the oxidation process.

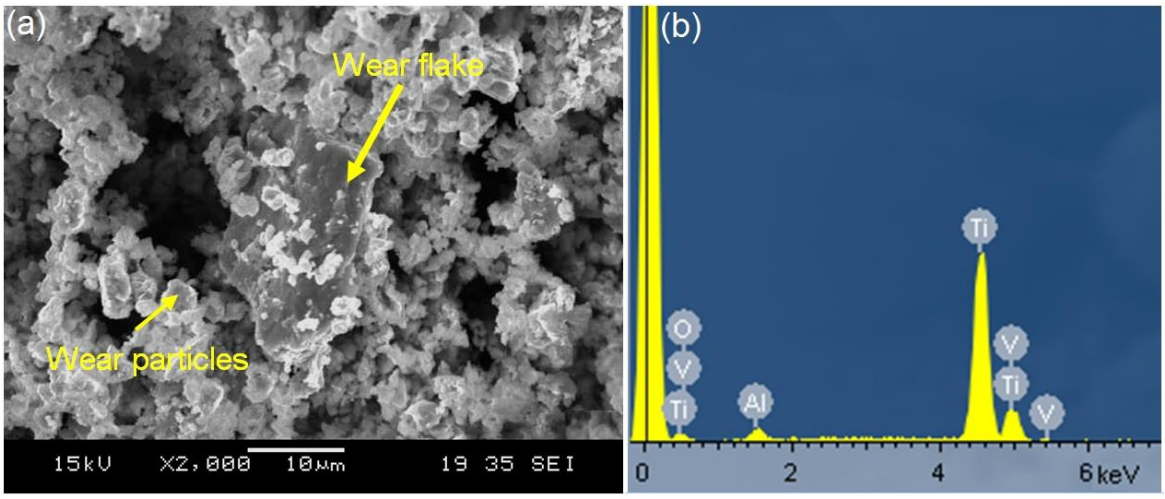

Fig. 16. (a) SEM micrograph of wear debris accumulated from wear track of HPCSTi64-Coat with SPP of 60psi tested dry and (b) EDX spectrum of wear flake.

Figure 16a shows the SEM micrograph of wear debris accumulated from the wear track of the HPCSTi64-Coat with the SPP of 60psi tested dry in which small wear particles and flakes are found. The small wear particles result from the abrasive wear of the HPCSTi64-Coat as the wear flakes probably come from the detachment of tribo-layers [3,10,11,28-30]. The O peak of the wear flake found on its EDX spectrum with Ti, Al and V peaks (Figure 16b) is indicative of its frictional-heat-induced-oxidation.

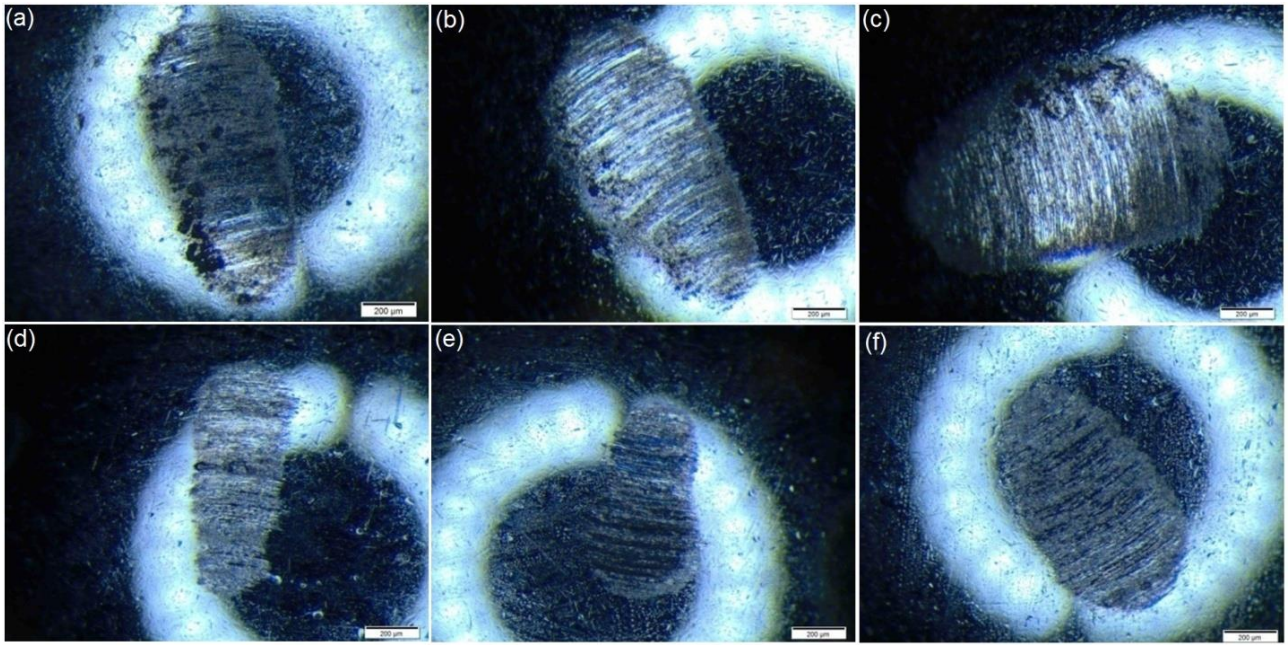

Figure 17: Wear morphologies of 100Cr6 steel balls rubbed on HPCSTi64-Coats with SPPs of (a and d) 0, (b and e) 10 and (c and f) 60psi (a-c) without or (d-f) with MOL.

Figures 17a-c show the wear scars of the steel balls rubbed on the HPCSTi64-Coats without or with SP under dry condition. The wear scars of the steel balls becomes larger with higher SPP because the rougher surface of the HPCSTi64-Coat serves as an abrading-surface for the higher abrasive wear of its counter steel ball. In addition, the higher wear resistance of the HPCSTi64-Coat associated with higher SPP is also responsible for the higher abrasive wear of its counter steel ball. Abrasive-lines on the wear scars confirm the abrasive wear of the steel balls as the counter steel balls have more apparent abrasive-lines on their wear scars for the HPCSTi64-Coats with SP than for the one without SP.

The steel balls lubricated with the MOL (Figures 17d-f) have apparently smaller wear scars compared to those tested without the MOL (Figures 17a-c). It is obvious that the MOL effectively lubricates not only the HPCSTi64-Coats but also their counter steel balls. Among the steel balls lubricated with the MOL (Figures 17d-f), the steel ball rubbed on the best bearing surfacce of the HPCSTi64-Coat with the SPP of 10psi has the smallest wear scar via the most effective lubrication with the MOL (Figure 17e). Under lubrication with the MOL, the counter steel ball has a larger wear scar for the SPP of 60psi (Figure 17f) than for the SPP of 10psi (Figure 17e) as the wear of the HPCSTi64-Coat with 60psi is higher than that of the one with 10psi. The effect of surface roughness of the HPCSTi64-Coat on the wear of its counter steel ball still can be found even under the lubrication condition.

4. CONCLUSION

The HPCSTi64-Coats were shot peened at the SPPs of 10-60psi to investigate changes in their structural, mechanical and tribological properties with SPP. The following conclusions were made.

- The higher SPP resulted in the higher protruded surface asperities of the HPCSTi64-Coats by forming the deeper surface dimples via the more energetic bombardment of steel shots. The surface analysis showed that the HPCSTi64-Coat with the SPP of 10psi had the best bearing surface among the HPCSTi64-Coats used in this study.
- The HPCSTi64-Coats with SP had the lower surface porosity levels than the one without SP.
- The surface hardness of the HPCSTi64-Coats increased with increased SPP via the enhanced cold work hardening.
- The wear of the HPCSTi64-Coats under dry condition decreased with increased SPP as a result of their increased surface hardness and thereby wear resistance. The HPCSTi64-Coats with SP had the better abrasive wear resistance than the one without SP under dry condition.
- The wear of the HPCSTi64-Coats lubricated with the MOL became higher with higher SPP because their bearing surfaces degraded with their increased surface roughness. The best bearing surface of the HPCSTi64-Coat with the MOL was found at the SPP of 10psi. Therefore, the HPCSTi64-Coat with 10psi had the lowest wear among the HPCSTi64-Coats tested with the MOL.
- The HPCSTi64-Coats lubricated with the MOL exhibited the lower wear than those tested without the MOL. The MOL was an effective lubricant for the HPCSTi64-Coats.
- The effects of SPP on the wear of the HPCSTi64-Coats and their counter steel balls were found.

Acknowledgement

Authors are grateful for the financial support from the National Research Foundation (NRF), Rolls-Royce (RR), and Nanyang Technological University (NTU), Singapore, with the NRF-RR-NTU research grant number of M-RT3.1, and the project team members from RR, Singapore, IulianMarinescu, Anna Tai, and Nicholas Weeks for their contributions in this project. Authors acknowledge Dr. Pham (Ho Chi Minh City University of Technology (HCMUT), VNU-HCM) for the shot peening experiment.

REFERENCES

[1] J.S. Rudas, L.M. Gomez, A. Toro, J.M. Gutierrez, A. Corz, *Wear rate and entropy generation sources in a Ti-6Al-4V/WC/100Co sliding pair*, Journal of Tribology, vol. 139, iss. 6, 2017, doi: 10.1115/1.4036321

[2] W.Y. Li, C. Zhang, X. Guo, J. Xu, C.J. Li, H. Liao, C. Coddet, K.A. Khor, *Ti and Ti-6Al-4V coatings by cold spraying and microstructure modification by heat treatment*, Advanced Engineering Materials, vol. 9, iss. 5, pp. 418-423, 2007, doi: 10.1002/adem.200700022

[3] N.W. Khun, W.Q. Toh. E. Liu, *Study on changes in hardness and wear resistance of 3D printed Ti-6Al4-V with repsect to heat treatment temperature*, Tribology in Industry, vol. 45, no. 1, pp. 129-135, 2023, doi: 10.24874/ti.1421.12.22.02

[4] N.W. Khun, A.W.Y. Tan, E. Liu, *Effect of working pressure on wear and corrosion resistance of cold sprayed Ti-6Al-4V coatings*, Surface and Coatings Technology, vol. 302, pp. 1-12, 2016, doi: 10.1016/j.surfcoat.2016.05.052

[5] J. Qu, P.J. Blau, T.R. Watkins, O.B. Cavin, N.S. Kulkarni, *Friction and wear of titanium alloys sliding against metal, polymer and ceramic counterfaces*, Wear, vol. 258, iss. 9. pp. 1348-1356, 2005, doi: 10.1016/j.wear.2004.09.062

[6] C. Leyens, H. Gedanitz, *Long-term oxidation of orthorhombic alloy Ti-22Al-25Nb in air between 650 and 800 ℃*, Scripta Materials, vol. 41, no. 8, pp. 901–906, 1999, doi: elib.dlr.de/17062/

[7] A. Ralison, G. Dettemwamger, M. Schutze, *Oxidation of orthorhombic Ti2AlNb alloys at 800 ℃ in air*, Materials and Corrosion, vol. 51, iss. 5, pp. 317–328, 2000, doi: 10.1002/(sici)1521-4176(200005)51:5%3c317::aid-maco317%3e3.0.co;2-w

[8] H. Singh, T.S. Sidhu, S.B.S. Kalsi, *Cold spray technology: Future of coating deposition processes*, Frattura ed Integrita Strutturale, vol. 6, no. 22, pp. 69-84, 2012, doi: 10.3221/IGF-ESIS.22.08

[9] S.V. Klinkov, V.F. Kosarev, M. Rein, *Cold spray deposition: Significant of particle impact phenomena*, Aerospace Science and Technology, vol. 9, iss. 7, pp. 582-591, 2005, doi: 10.1016/j.ast.2005.03.005

[10] N.W. Khun, P.Q. Trung, D.L. Butler, *Mechanical and tribological properties of shot peened SAE1070 steel*, Tribology Transactions, vol. 59, iss. 5, pp. 932-943, 2016, doi: 10.1080/10402004.2015.1121313

[11] N.W. Khun, P.Q. Trung, D.L. Butler, *Study on hardness and wear resistance of shot peened AA7075-T6 aluminium alloy*, Engineering Research Express, vol. 3, iss.1, 2021, doi: 10.1088/2631-8695/abea0a

[12] M.F. Fernandes, M.A.S. Torres, M.P.C. Fonseca, C.A.R.P. Baptista, *Investigation of residual stress, stress relaxation and work hardening effects induced by shot peening on the fatigue life of AA6005-T6 aluminum alloy*, Materials Research Express, vol. 6, iss. 12, 2020, doi: 10.1088/2053-1591/ab6c8f

[13] H.Y. Miao, D. Demers, *Experimental study of shot peening and stress peen forming*, Journal of Materials Processing Technology, vol. 210, iss. 15, pp. 2089-2102, 2010, doi: 10.1016/j.jmatprotec.2010.07.016

[14] O. Evtushenko, M. Kazachenok, D. Buslovich, S. Martynov, *Effect of oxidation on wear resistance of 3D printed titanium alloy Ti6Al4V parts*, AIP Conference Proceedings, vol. 2167, iss. 1, pp. 020094, 2019, doi:10.1063/1.5131961

[15] D.V. Girish, M.M. Mayuram, S. Krishnamurthy, *Surface integrity studies on shot peened thermal treated EN24 steel spur gears*, Wear, vol. 193, iss. 2, pp. 242-247, 1996, doi: 10.1016/0043-1648(95)06791-4

[16] D.L. Butler, *The three dimensional surface topographic characterization of diamond grinding wheels*, Advanced Materials Research, vol. 126-128, pp. 690-695, 2010, doi: 10.4028/www.scientific.net/AMR.126-128.690

[17] D.L. Butler, L.A. Blunt, B.K. See, J.A. Webster, K.J. Stout, *The characterization of grinding wheels using 3D surface measurement techniques*, Journal of Materials Processing Technology, vol. 127, iss. 2, pp. 234-237, 2002, doi: 10.1016/S0924-0136(02)00148-6

[18] M. Karimi, B. Jodoin, G. Rankin, *Shock wave induced spraying: Modeling and physics of a new spray process*, Journal of Thermal Spray Technology, vol. 20, iss. 4, pp. 866-881, 2011, doi: 10.1007/s11666-011-9622-4

[19] H. Katanoda, T. Matsuoka, K. Matsuoka, *Experimental study on shock wave structures in constant-area passage of cold spray nozzle*, Journal of Thermal Spray Technology, vol. 16, iss. 1, pp. 40-45, 2007, doi: 10.1007/s11630-007-0040-3

[20] K. Zhan, C.H. Jiang, X.Y. Wu, V. Ji, *Surface layer characterization of S30432 austenite stainless steel*, Materials Transactions vol. 53, iss. 5, pp. 1002-1006, 2012, doi: 10.2320/matertrans.m2011390

[21] A.P.A. Manfridini, C. Godoy, J.C.A.B. Wilson, M.V. Auad, *Surface hardening of IF steel by plasma nitriding: Effect of a shot peeing pretreatment*, Surface and Coatings Technology, vol. 260, pp. 168-178, 2014, doi: 10.1016/j.surfcoat.2014.09.064

[22] F. Svahn, A.K. Rudolphi, E. Wallén, *The influence of surface roughness on friction and wear of machine element coatings*, Wear, vol. 254, iss. 11, pp. 1092-1098, 2003, doi: 10.1016/S0043-1648(03)00341-7

[23] P.L. Menezes, Kishore, S.V. Kailas, *Influence of surface texture and roughness parameters on friction and transfer layer formation during sliding of aluminium pin on steel plate*, Wear, vol. 267, iss. 9-10, pp. 1534-1549, 2009, doi: 10.1016/j.wear.2009.06.003

[24] T. Goyal, R.S. Walia, T.S. Sidhu, *Surface roughness optimization of cold sprayed coatings using Taguchi method*, International Journal of Advanced Manufacturing Technology, vol. 60, iss. 5, pp. 611-623, 2012, doi: 10.1007/s00170-011-3642-6

[25] F. Liu, Z.M. Jin, C. Rieker, R. Oberts, P. Grigoris, *Effect of wear of bearing surfaces on elastohydrodynamic lubrication of metal-on-metal hip implants*, Proceedings of the Institution of Mechanical Engineers, Part H: Journal of Engineering in Medicine, vol. 219, iss. 5, pp. 319-3128, 2005, doi: 10.1243/095441105x34356

[26] L. Mattei, F.D. Puccio, B. Piccigallo, E. Ciulli, *Lubrication and wear modelling of artificial hip joints: A review*, Tribology International, vol. 44, iss. 5, pp. 532-549, 2011, doi: 10.1016/j.triboint.2010.06.010

[27] J. Awrejcewicz, P. Olejnik, *Occurrence of stick-slip phenomenon*, Journal of Theoretical Applied Mechanics, vol. 45, no. 1, pp. 33-40, 2007.

[28] M.M. Khruschov, *Principal of abrasive wear*, Wear, vol. 28, iss. 1, pp. 69–88, 1974, doi: 10.1016/0043-1648(74)90102-1

[29] S.B. Pitchuka, B. Boesl, C. Zhang, D. Lahiri, A Nieto, G. Sundararajan, A. Agarwal, *Dry sliding wear behavior of cold sprayed aluminum amorphous/nanocrystalline alloy coatings*, Surface and Coatings Technology, vol. 238, pp. 118-125, 2014, doi: 10.1016/j.surfcoat.2013.10.055

[30] C.J. Li, H.T. Wang, G.J. Yang, C. G. Bao, *Characterization of high temperature abrasive wear of cold sprayed FeAl intermetallic compound coating*, Journal of Thermal Spray Technology, vol. 20, iss. 1-2, pp. 227-233, 2011, doi.or./ 10.1007/s11666-010-9545-5

[31] J. Meng, N.H. Loh, B.Y. Tay, G. Fu, S.B. Torr, *Tribologicalbehaviour of 316L stainless steel fabricated by micro powder injection molding*, Wear, vol. 268, iss. 7-8, pp. 1013-1019, 2010, doi: 10.1016/j.wear.2009.12.033